Effects of Dipole Moment and Temperature on the Interaction Dynamics of Titania Nanoparticles during Agglomeration

Wen Yan, Shuiqing Li,* Yiyang Zhang, and Qiang Yao

Key Laboratory for Thermal Science and Power Engineering of Ministry of Education, Department of Thermal Engineering, Tsinghua University, Beijing 100084, China

Stephen D. Tse

Department of Mechanical and Aerospace Engineering, Rutgers University, Piscataway, New Jersey 08854

Received: March 26, 2010; Revised Manuscript Received: May 7, 2010

The interactions between nanoparticles in high-temperature vapor-synthesis environments have important implications on their self-assembly into specific structures. We apply classical molecular dynamics (MD) simulations, with the Matsui−Akaogi interatomic potential, to study the interaction forces and the resulting dynamics between pairs of cooriented and counteroriented charge-neutral TiO_2 anatase nanoparticles in vacuum. The distributions of Ti and O ions at the nanocrystal surface are asymmetric due to limited surface sites preventing perfect sphericity, resulting in permanent dipoles that are approximately proportional to the surface area in magnitude. For two approaching cooriented nanoparticles, with parallel dipole moments, the nanoparticles translate toward each other with minimal rotation, where the attractive Coulomb dipolar force is much larger than the van der Waals force at long-range distances. For two approaching counteroriented nanoparticles, with antiparallel dipole moments and initially repulsive interaction, the nanoparticles experience mutual rotations, and the Coulomb force changes from repulsive to attractive during translation. Both the Hamaker approximation and the dipole−dipole approximation are compared with the MD simulation results to assess their validity as a function of particle separation distance. As the temperature increases from 273 to 1673 K, the fluctuation of the dipole vector (in both magnitude and direction) increases, resulting in a dramatic decrease of the time-averaged dipole moment from 60 to 2.1 D, as well as a reduction of the Coulomb dipolar force between the two nanoparticles.

I. Introduction

Understanding and predicting the roles of intrinsic forces between nanoparticles (NPs) has received a great deal of attention, driven by both scientific and technological needs in a wide range of fields, such as materials science (sintering and agglomeration),[1,2] atmospheric science (aerosol coagulation),[3] chemical engineering (colloidal dispersion),[4,5] and astrophysics (planet formation).[6] For example, in colloidal systems, substantial efforts have been focused on the van der Waals (vdW) interactions of small particles that originate from irreducible fluctuations of electromagnetic (EM) fields in a vacuum.[7−10] A rigorous treatment of the vdW interactions for two infinite half-spaces was pioneered by Lifshitz on the basis of fluctuational electrodynamics.[11] Evaluation of the vdW force between nano- or microsized particles often relies on the approximation of pairwise forces within the simpler Hamaker formulation. Elements of the Lifshitz theory for half-spaces can be incorporated within the Hamaker approach to obtain a semiempirical relation for the vdW force between two particles.[7,10]

Recent molecular dynamics (MD) simulations have shown that the Coulombic interaction of fluctuating dipoles is the dominant mechanism of heat transfer between nanoparticles.[12,13] It has been reported that both vdW interaction and radiative heat transfer between NPs are related to near-field effects due to tunneling of evanescent waves.[14,15] However, study of the contribution of Coulombic forces due to existing dipole moments (permanent or induced) of NPs, rather than dispersive vdW forces, on the total interparticle interaction is limited. Interestingly, it has been found that permanent dipoles exist in semiconductor nanocrystals (NCs) such as CdSe NCs with a wurzite structure[16,17] and ZnSe NCs with a centrosymmetric lattice.[18] Moreover, the NP dipole is considered to be an important factor responsible for the self-assembly of NP functional nanostructures.[19] For example, for CdSe NPs in the presence of both dispersive (vdW) and dipolar−dipolar force fields, short-range vdW forces favor their formation into close-packed structures, whereas dipolar−dipolar interactions allow for their arrangement into more open structures, such as quasi-dimensional chains.[20,21]

Recently, interests in synthesizing ultrafine, high-purity anatase titania particles (e.g., TiO_2) with sizes < 10 nm have dramatically increased as they are expected to play important roles in addressing various environmental and energy challenges due to their unique properties (e.g., as a photocatalyst and photosensitizer, respectively) applicable for wastewater remediation and solar energy conversion.[22] The synthesis methods include wet-chemical, chemical vapor deposition, and flame synthesis, with gas-phase flame hydrolysis of $TiCl_4$ being the major production route.[23] The agglomeration and sintering of primary TiO_2 NPs, in the presence of both dispersive vdW and Coulomb dipolar interactions, as mentioned above, affect the morphology of flame-made titania products, impacting their photocalytic and photovoltaic applications.[24−26] Therefore, it is

* To whom correspondence should be addressed. Fax: +86-10-62773384. E-mail: lishuiqing@tsinghua.edu.cn.

10.1021/jp102750k
Published on Web 05/28/2010

TABLE 1: Interaction Parameters for the Matsui−Akaogi Potential[a]

	q	A	B	C
Ti	2.196	1.1823	0.077	22.5
O	−1.098	1.6339	0.117	54.0

[a] Units: q in |e|, A and B in Å, and C in Å^3 kJ$^{0.5}$ mol$^{-0.5}$.

critical to understand interactions between TiO_2 NPs during agglomeration. However, there are few reports found in the literature on the dipole properties of metal-oxide-type NPs like TiO_2, with even fewer discussing characterization of the dipole moment in relation to particle size. Furthermore, with the dipoles of NPs undergoing significant thermal fluctuations in high-temperature environments such as flame aerosol reactors, the influence of temperature on Coulombic dipolar interactions, as well as the overall interactions of NPs, is still unclear and needs further investigation.

This paper aims to clarify the detailed contributions of dispersive vdW and Coulombic dipolar forces in the interaction of two approaching anatase TiO_2 NPs, for different particle sizes and initial particle temperatures. The simple Hamaker approximation and the dipole−dipole approximation models are compared with the MD simulation results.

II. Methods

The Matsui−Akaogi (MA) potential,[27] which has been validated by X-ray absorption spectra data to be one of most suitable force fields for TiO_2 structures,[28,29] is employed here to describe the interaction of atoms. In the MA potential, the interaction energy U_{ij} between atoms i and j separated by a center-to-center distance of r_{ij} is expressed as

$$U_{ij} = \frac{q_i q_j}{r_{ij}} - \frac{C_i C_j}{r_{ij}^6} + f(B_i + B_j)\exp\left(\frac{A_i + A_j - r_{ij}}{B_i + B_j}\right) \quad (1)$$

where the three terms on the right-hand side of the equation represent electrostatic (Coulomb), dispersion (vdW), and repulsion interactions, respectively. The last two terms constitute a Buckingham potential. The values of partial charges q and the parameters A, B, and C of atom i (or j) in eq 1 are listed in Table 1.

Molecular dynamics (MD) simulations are performed using the DL-POLY code (version 2.18)[30,31] with the MA potential to understand the interaction dynamics between two identical approaching TiO_2 NPs with diameters of 2, 3, 4, and 5 nm. Generally, the complete interactions between two NPs include a precontact approach process followed by an on-contact sintering (coalescence) process. As for the on-contact sintering process, where grain boundary diffusion and surface diffusion are predominant, several MD simulation studies have been conducted.[1,29] In this work, we investigate the precontact approach and isolate the respective roles of Coulomb and vdW forces. Surprisingly, such a study has received relatively little attention, despite its importance in understanding NP self-assembly and aggregation in synthesis processes.[32]

The simulation procedure of this work is given as follows. First, a perfect lattice is constructed using parameters for anatase, given that the anatase phase dominates for TiO_2 nanocrystals with $d_p < 10$ nm. Then, a spherically circumscribed NP with a set diameter is "excised" from the lattice. We term it as NP1. The excess titanium or oxygen ions are removed from NP1 to maintain electrical neutrality. Next, the neutral NP1 is simulated in the canonical ensemble (NVT) for at least 3 ns (600 000 5-fs time steps), which is sufficient for equilibration at the given temperature. This equilibration state has been shown by repeated tests to be independent of the initial MD velocity distribution. The dipole moment, $\mathbf{p}$, of a NP is calculated by $\mathbf{p} = \sum_i q_i \mathbf{r}_i$, where q_i and $\mathbf{r}_i$ are the charge and position vector of ion i (either titanium or oxygen), respectively. Finally, the configuration of NP1 is replicated and translated along the x-axis to establish two particles separated by a center-to-center distance equal to 10 times the nanoparticle diameter (e.g., 30 nm for a 3 nm NP). We term it as NP2. NP2 is given one of two possible orientations initially; one keeps the same lattice orientation as NP1 (cooriented mode), and the other rotates the particle by an angle of π around its centroid to obtain a dipole direction opposite (antiparallel) to that of NP1 (counteroriented mode). Collision of the two nanoparticles is investigated using the microcanonical ensemble (NVE) by setting one particle with an initial velocity of 10 m/s (based on the order of magnitude of Brownian motion of the nanoparticles for our cases) while the other one is fixed with zero initial velocity. The simulation is run for 3 ns (3 000 000 1 fs time steps), which is of sufficient duration to bring them into contact but not enough to study the entire sintering process. This procedure is repeated for nanoparticles with diameters of 2, 3, 4, and 5 nm and initial NVE temperatures of 273, 973, 1273, 1473, 1673, 2473, and 2673 K, respectively, to investigate the effect of temperature on interparticle interactions with different diameters.

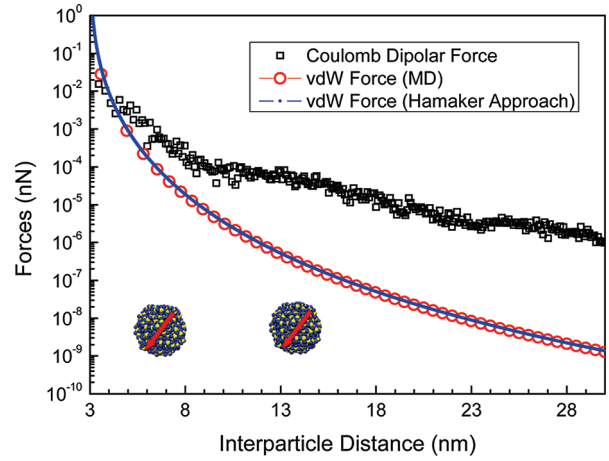

Figure 1. Interaction forces between two cooriented 3 nm TiO_2 nanoparticles during the approaching process. The decomposition of interparticle forces into the vdW and Coulomb components naturally corresponds to their Coulomb and dispersion terms of Matsui−Akaogi potentials between all atoms.

III. Results and Discussion

III.1. Interaction Forces between Two TiO_2 NPs. Figure 1 shows the interaction forces between two approaching 3 nm cooriented anatase TiO_2 NPs at 273 K as a function of the interparticle center-to-center distance (hereinafter referred to as X_{12} for NP1 and NP2). The interparticle forces can be decomposed into Coulomb, vdW, and repulsive components, which are related by derivatives to their respective MA interatomic potential terms in eq 1. The total interaction energy is obtained by integrating these three terms for all atoms in the two NPs. Comparatively, in precontact approach (namely, with X_{12} larger than one particle diameter), the repulsion forces between two NPs can be neglected since they have values that are several orders of magnitude lower than the Coulomb and

vdW forces. The vdW force, which originates from the interaction of the dynamic (time-dependent) dipoles,[33] is attractive and increases smoothly as the two NPs approach each other. Generally, the charge density of small particles, even if electrically neutral, includes not only a dynamic dipole but also a static one.[33] The Coulomb force between two NPs, obtained from the summation of the MA Coulomb potentials of the titanium and oxygen ions, is not zero, exhibiting attractive behavior and increasing with decreasing X_{12}. The nonzero Coulomb force implies that the 3 nm TiO_2 NP should have a static permanent dipole (more discussion later). As shown in Figure 1, the Coulomb force, which is sensitive to the detailed atomic structure of the NPs, fluctuates significantly due to thermal vibrations of the titanium and oxygen ions. The Coulomb force between two cooriented NPs exhibits attractive behavior and is much larger than the vdW force by several orders of magnitude at long X_{12}, for example, about three orders for $X_{12} = 15-30$ nm, two orders for $X_{12} = 10-15$ nm, and one order for $X_{12} = 4-10$ nm. However, as X_{12} continues to decrease, the vdW force increases more rapidly than the Coulomb force, nearly catching up at $X_{12} = 4.0$ nm. As X_{12} becomes smaller than 4.0 nm, the vdW force exceeds the Coulomb force, but they are still both comparable in magnitude. For instance, in the interval $X_{12} = 3.0-4.0$ nm, the Coulomb force is an average of about 0.6 times the vdW force.

Since the vdW potential between two atoms varies as $U_{ij} \propto -C_iC_j/r_{ij}^6$, as shown in eq 1, the approximate Hamaker approach, obtained by a simple pairwise summation of the vdW potential between atoms, can be used to predict the vdW interaction energy between two spherical nanoparticles, NP1 and NP2, as given below[20,34]

$$W_{12}^{\mathrm{vdW}} = -\frac{A}{12}\left(\frac{4R^2}{D_{12}^2 + 4D_{12}R} + \frac{4R^2}{D_{12}^2 + 4D_{12}R + 4R^2} + 2\ln\left(\frac{D_{12}^2 + 4D_{12}R}{D_{12}^2 + 4D_{12}R + 4R^2}\right)\right) \quad (2)$$

where R is the radius of a NP and $D_{12} = (X_{12} - 2R)$ is the separation distance of the closest approach between NP1 and NP2. The Hamaker constant A is given as

$$A = \pi^2\overline{(C_iC_j)_\Sigma}\rho_1\rho_2 \quad (3)$$

where ρ_1 (or ρ_2) is the number density of the atoms contained in NP1 (or NP2). $\overline{(C_iC_j)_\Sigma}$ is the averaged dispersion coefficient of all atoms in NP1 and NP2, which can be estimated from the vdW term of the MA potential of eq 1 using the parameters for TiO_2 in Table 1. In this work, we calculate A to be 240.5 zJ (1 zJ = 10^{-21} J) for anatase TiO_2 and 287.0 zJ for rutile TiO_2. This value for anatase TiO_2 agrees reasonably well with the value of 199.0 zJ given by the single oscillator approximation and the value of 173.1 zJ given by the full spectral method,[35] particularly considering the uncertainty in the measurement and estimation of the Hamaker constant in the vacuum system.

The vdW force between NP1 and NP2 can also be approximated by taking the derivative of the corresponding term in eq 1, that is, $F_{12} = -\mathrm{d}W/\mathrm{d}D_{12}$. A comparison between the vdW force obtained by the Hamaker approximation and that obtained by the MD simulation is also illustrated in Figure 1. These two predictions are found to nearly coincide for $X_{12} > 4.0$ nm, with the prediction error less than 30% for the Hamaker approximation. As X_{12} is reduced further, the discrepancy increases, being more than 10 times different at $X_{12} = 3.1$ nm (or $D_{12} = 0.1$ nm). This difference is to be expected since at close contact, the shape changes of NPs differ substantially from the perfect sphere assumed in the Hamaker approximation.

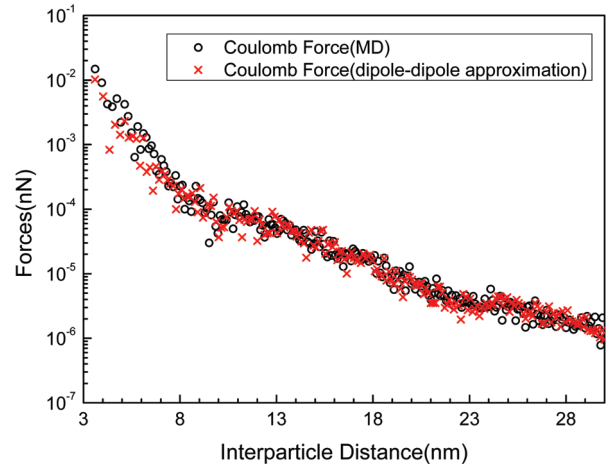

Figure 2. Comparison of interparticle Coulomb forces predicted by both the MD simulation and the approximate dipole−dipole model for the 3 nm nanoparticles of Figure 1.

As the nanoparticles are electrically neutral, the Coulomb force between them, shown in Figure 1, can be thought of as a Coulomb dipole−dipole interaction, leading to formation of a static permanent dipole on the nanoparticles.[18−20] This permanent dipole may be attributed to the asymmetric distribution of titanium and oxygen ions at the surface since a nanocrystal lattice cannot be conformed into a perfect sphere due to a limited number of surface ions of fixed positions. For a single "spherically-shaped" NP, the geometrical center of all positive ions is found not to coincide exactly with that of all negative ions, with the difference being proportional to the strength of the permanent dipole. For the 3 nm anatase TiO_2 NP at 273 K, the MD simulation predicts a mean distance between the centers of the positive ions and negative ions of 0.0014 nm, providing the NP a permanent dipole of about 60D as given by the formula $\mathbf{p} = \sum_i q_i\mathbf{r}_i$. As a result, the Coulomb interaction energy between NP1 and NP2 can be expressed by the dipole−dipole approximation given below[36]

$$W_{12}^{\mathrm{d-d}} = \frac{1}{4\pi\varepsilon_0}\frac{\mathbf{p}_1\cdot\mathbf{p}_2 - 3(\mathbf{n}\cdot\mathbf{p}_1)(\mathbf{n}\cdot\mathbf{p}_2)}{X_{12}^3} \quad (4)$$

where X_{12} is the interparticle center-to-center distance, defined as $X_{12} = |X_1 - X_2|$, and $\mathbf{n}$ is the unit vector in the direction $(X_1 - X_2)$. Similarly, the Coulomb dipolar force between two NPs can be obtained by taking the derivative of eq 4.

Figure 2 compares the Coulomb forces predicted by the MD simulation and the dipole−dipole approximation model for the 3 nm particles of Figure 1. In calculating the force in the dipole−dipole approximation, the permanent dipole ($\mathbf{p} = \sum_i q_i\mathbf{r}_i$) of the NPs are updated in time using the MD simulated coordinates of all ions, $\mathbf{r}_i$. At a long distance of $X_{12} > 6$ nm, the dipole−dipole model gives a fairly good approximation to the MD results. For instance, in the interval of $30 > X_{12} > 6$ nm, the force ratio of the dipole−dipole approximation to the MD simulation fluctuates within the range of 1.0 ± 0.4. The larger X_{12}, the smaller the difference between the two models. For $6 > X_{12} > 3.2$ nm, the prediction of the dipole−dipole model is

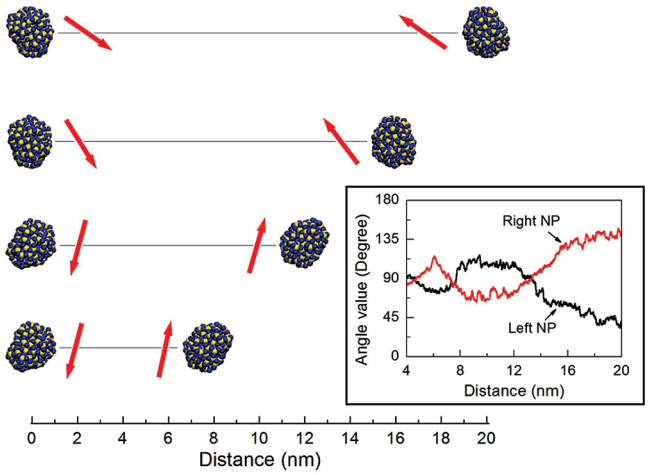

Figure 3. Snapshots of two counteroriented nanoparticles showing the varied directions of their dipoles during the approaching process.

generally less than that of the MD results, with the force ratio within the range of 0.6 ± 0.4. For $X_{12} < 3.2$ nm, the force ratio is 1 or 2 orders of magnitude. Thus, the Coulomb force between NPs during precontact approach can be attributed mainly to the role of particle dipoles, except for in the close-contact zone of $X_{12} < 3.2$ nm (or $D_{12} < 0.2$ nm).

For two NPs that are cooriented with the same dipole directions, as shown in Figures 1 and 2, they experience very weak rotation during their approach from long distance to close contact. To study the orientation effect of NP dipoles, the case of two counteroriented NPs during the approaching process is examined, as illustrated in Figure 3 by using Visual Molecular Dynamics.[37] The arrows show the directions of the dipoles of NP1 (left) and NP2 (right), and the inset plots the absolute value of the angle, θ_d, between the NP dipole and the x-axis as a function of the particle separation distance. Initially, at $X_{12} =$ 20 nm, the absolute θ_d of NP1 and NP2 are 30 and 150°, respectively. Upon translation, both NP1 and NP2 begin to rotate clockwise. Approaching $X_{12} = 13$ nm, the absolute θ_d of NP1 and NP2 are both approximately 90° but at opposite dipole direction. As X_{12} further decreases from 13 to 4 nm, the absolute θ_d of the two NPs precesses twice at around 90°. Finally, for $X_{12} < 4$ nm, they become nearly settled at 90°. Through the whole process, the sum of the two angle values of the dipoles is constant at 180°, with NP1 and NP2 always maintaining antiparallel dipoles during their approach, satisfying the principle of minimum Coulomb interaction energy according to eq 4. It should be noted that the dipole−dipole interaction between the two counteroriented NPs is initially repulsive. During the approach, as induced by the inertial movement of NP2, the aforementioned rotations of the NPs make their interaction attractive at about $X_{12} = 15$ nm.

III.2. Characteristics of the Dipole of a Single TiO_2 NP. The determination of the permanent dipole of a NP plays a key role in the particle-level macroscopic approach describing the interaction of two NPs. A MD simulation of a single 3 nm anatase TiO_2 NP is conducted in the NVE ensemble for 3 ns at both 273 and 1673 K. Figure 4 shows the variation of the magnitude of the NP dipole moment as a function of the time. At 273 K, it fluctuates in a range from 40 to 80 D. Additionally, the projection of the dipole direction varies in an angle range of about $\pi/4$ (see inset A of Figure 5). At 1673 K (e.g., for that found in high-temperature flame reactors), the magnitude of the NP dipole moment fluctuates more significantly, ranging from 6 to 100 D. Also, the direction of the dipole varies in a wider

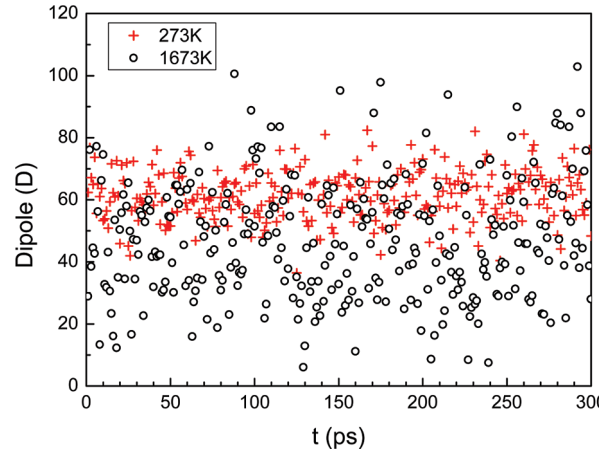

Figure 4. Time evolution of the dipole moment of a 3 nm TiO_2 particle in an NVE ensemble at 273 and 1673 K.

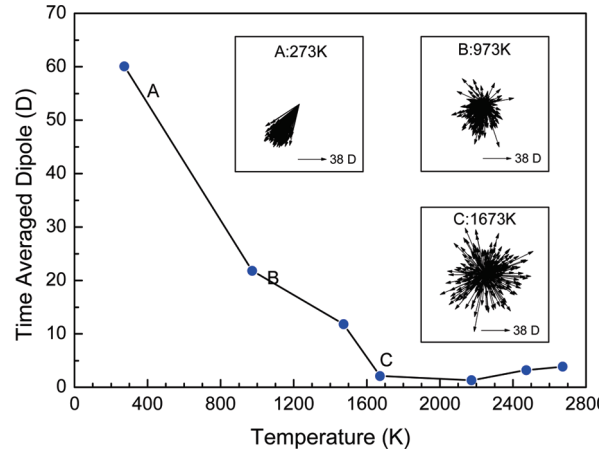

Figure 5. Time-averaged dipole moments of a TiO_2 nanoparticle at different temperatures. Insets A, B, and C show the distribution of dipole vectors projected onto the $x-y$ plane along the time period at different temperatures.

angle range of nearly 2π (see inset C of Figure 5). The fluctuating dipole moment vector leads to the fluctuating Coulomb forces between the NPs (as shown in Figure 1) and can be associated with the vibration of the atoms in the lattice. Reports on the dipole of a TiO_2 spherical NP are scarce. There are some referenced data on semiconductor NPs such as CdSe and ZnSe, as observed by dielectric dispersion measurements.[16,18] For bulk polar CdSe, the dipole moments of 3.4 and 4.6 nm CdSe nanocrystals are 25 and 47 D, respectively. Although ZnSe has no bulk dipole due to its centrosymmetric lattice, a 3.3 nm ZnSe nanocrystal has a dipole moment of about 42 D.[18] These values of dipole moment are of the same magnitude as that for the 3 nm TiO_2 NP predicted by our MD simulation. It is known that bulk anatase TiO_2 has no dipole despite its noncentrosymmetric lattice. As a result, we deduce that the origin of the dipole in the anatase TiO_2 NP arises from the previously described asymmetric distribution of ions at the surface of the NP, similar to the origin of the dipole moment in PbSe nanocrystals, which is attributed to the noncentrosymmetric arrangement of Pb- and Se-terminated {111} facets.[20,21]

III.3. Influence of System Temperature. Since NPs experience high temperatures during gas-phase synthesis, we study a single 3 nm TiO_2 NP at different temperatures via simulation in NVE for 300 ps. The time-averaged dipole moment is readily obtained from the fluctuating moment data (e.g., Figure 4). Figure 5 shows the effect of temperature on the dipole of the

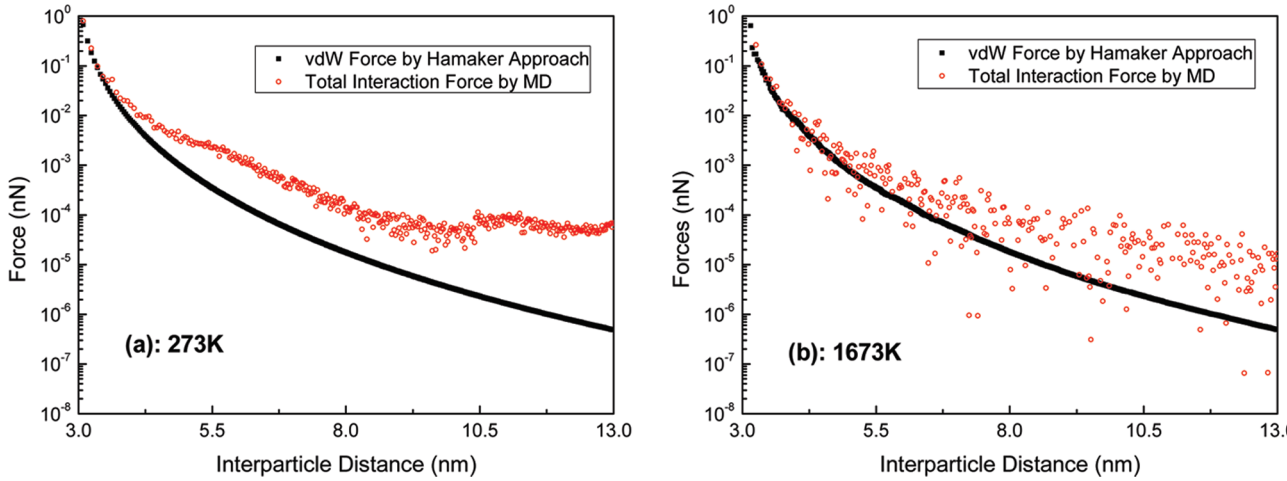

Figure 6. Evolution of the total interacting force and the vdW force between two 3 nm TiO_2 nanoparticles during the approaching process (a) with an initial temperature of 273 K and (b) with an initial temperature of 1673 K.

TiO_2 NP. As the temperature increases from 273 to 1673 K, the magnitude of the time-averaged dipole moment dramatically decreases from 60.1 to 2.1 D. As the temperature further increases, it remains below 4.0 D with relatively small deviation. The decrease of the magnitude of the time-averaged dipole moment with respect to temperature can be attributed to the increasing fluctuation of the instantaneous dipole direction. Inset A of Figure 5 shows the distribution of dipole vectors projected onto the $x-y$ plane for the given simulation time period at 273 K. The distribution of the fluctuating dipole directions is relatively narrow and is nearly constrained in the angle range of $\pi/4$. As the temperature increases to 973 K (inset B of Figure 5), the direction of the dipole vector spreads more widely, but the distribution is still obviously asymmetrical, resulting in a value of 21.8 D. When the temperature further increases to 1673 K (inset C of Figure 5), despite variance in dipole modulus, the spreading of the direction of the dipole vectors over the entire angular range makes the time-averaged dipole moment diminutive. The large fluctuations of the positions of the Ti and O ions in the lattice at high temperature generate a wide distribution of dipole directions according to $\mathbf{p} = \sum_i q_i \mathbf{r}_i$.

Ostensibly, the dipole changes under high temperature may affect the Coulomb dipolar force between two NPs. Figure 6 shows the vdW force (Hamaker) and the total interaction force (vdW + Coulomb + repulsive) between two cooriented approaching 3 nm TiO_2 NPs at 273 (left) and 1673 K (right). In the left plot, at an initial temperature of 273 K, prior to the repulsive force playing a role at close contact, the total interaction force is always larger than the vdW force, even by several orders of magnitude at certain X_{12}, given the strong attractive Coulomb dipolar force, with the NP dipole at around 60 D. However, at an initial temperature of 1673 K (right plot), the values of the total interaction force spread through the "smooth" values of the vdW force, indicating that the Coulomb dipolar force vacillates between being attractive and repulsive along the time evolution due to large fluctuations of the dipole direction at high temperature. For X_{12} ranging from 6 (i.e., one diameter separation) to 3.2 nm (i.e., 1/15 diameter separation), the interaction force is expected to play a key role in the self-assembly of NPs. However, in this range, the mean total interaction force is approximately that of the vdW force, washing out a net Coulombic force. Therefore, we conclude that preferential self-assembly at high temperatures is likely inhibited.

III.4. Influence of Particle Diameter. Figure 7 displays the effect of NP diameter on the time-averaged dipole moment at

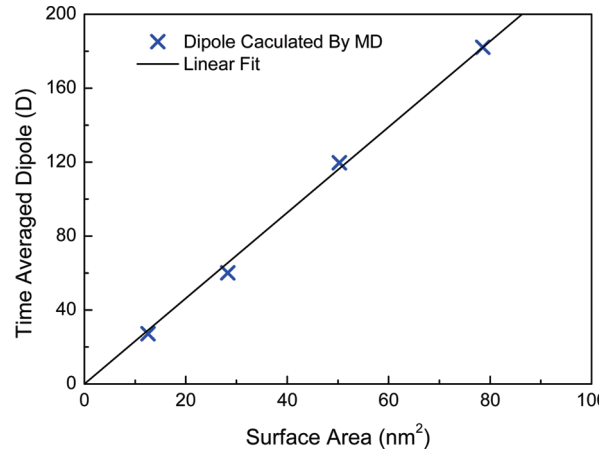

Figure 7. Time-averaged dipole moments as a function of the surface area of nanoparticles at a temperature of 273 K.

273 K. The dipole moment is found to be approximately proportional to the surface area ($\sim R^2$) of the spherically shaped TiO_2 NP. As the particle diameter increases from 2 to 5 nm, the surface area increases from 12.8 to 78.5 nm^2, corresponding to a linearly increasing dipole moment from 27.2 to 182.1 D. Interestingly, in previous work examining the size effect on the dipole of CdSe nanocrystals, Shim and Guyot-Sionnest[18] found that wurtzite CdSe exhibits a large permanent dipole moment that is linearly dependent on the core radius of the nanocrystal. They attributed this linear size dependence of the dipole moment to the nanocrystal facets being decorated with surface charges in the Se-hole states. On the other hand, Li and Alivisatos[17] found the dipole moment of CdSe nanorods to be linearly proportional to their volume ($\sim R^3$), where they associated the intrinsic polarity of the CdSe crystallographic lattice to the lack of inversion symmetry. Since bulk anatase TiO_2 is nonpolar, the linear surface area dependence of the NP dipole moment may be attributed to the asymmetric distribution of Ti and O ions at the surface of the particle surface. For example, nanocrystals decorated with N randomly placed surface charges lead to a dipole that scales as $N^{1/2}R$. Shim and Guyot-Sionnest[18] assumed that the presence of more than one charge will be strongly hindered by the large Coulomb interaction and hence lead to the limitation of one charge per facet ($N \approx 1$), causing the dipole to grow linearly with size ($\sim R$). However, in this work, we believe that the number N might be limited by the total number of surface sites, thus resulting in a dipole with

surface area ($\sim R^2$) dependence. It is worth noting that we expect this surface area dipole dependence to be valid only for our specific nanometer-size range, with a turning point in the trend, as larger particles (e.g., those of micrometer size) can possess increasing sphericity with more available surface sites for the ions, thereby producing more symmetric distributions with ever smaller dipole moments.

IV. Conclusions

The interaction forces between two anatase TiO_2 NPs are studied using classical MD simulations on the basis of the Matsui−Akaogi potential. During the approach stage, the Coulomb dipolar force between two 3 nm cooriented NPs is almost always attractive, being several orders of magnitudes larger than the vdW force for large X_{12} but dropping below the vdW force at $X_{12} = 4.0$ nm. The Hamaker approximation predicts the vdW forces, as compared to MD, by an error of less than 30% for $X_{12} > 4.0$ nm. The dipole−dipole approximation for the Coulomb force is nearly the same as that found in the MD simulations for $X_{12} > 6.0$ nm. Nevertheless, at a close range of $X_{12} < 3.2$ nm (or $D = 0.2$ nm), the two approximations can have prediction errors of several orders. For the approach of two 3 nm counteroriented NPs, the dipole−dipole interaction induces clockwise rotation for both NPs, eventually settling when the absolute angle between the dipole vector and the particle center-to-center axis is about perpendicular. During this process, initial repulsion changes to attraction as the NPs move toward each other. The permanent dipole of a spherical TiO_2 NP can be associated with the asymmetric distribution of both Ti and O ions at its surface, fluctuating at around 60 D for a 3 nm anatase TiO_2 due to the lattice vibration. The NP dipole moments are found to be approximately proportional to the surface area of spherically shaped TiO_2, that is, the square of the particle radius ($\sim R^2$) for these nanometer-size ranges. Thermal fluctuations cause the angular direction of the NP dipole vector to spread more widely. As a result, as the temperature increases from 273 to 1673 K, the time-averaged dipole dramatically reduces from 60 to 2.1 D, producing weakened Coulomb dipolar interactions between two TiO_2 NPs at high temperature. These results have implications on the self-assembly of functional nanostructures in high-temperature synthesis processes.

Acknowledgment. This work was mainly supported by the National Natural Science Fund of China (No. 50776054) and the National Program for New Century Excellent Talents in University and partially by the U.S. National Science Foundation (Grant No. CBET-0755615) for coauthor S.D.T. We acknowledge Dr. Koparde at Vanderbilt for kindly delivering his Ph.D. thesis to us. Thanks are due to Prof. Gang Chen at MIT and to Prof. Jeff Marshall at the University of Vermont for stimulating and helpful discussions. The helpful work of Mr. Junjing Wang and Ms. Sili Deng is appreciated.

References and Notes

(1) Hawa, T.; Zachariah, M. R. *Phys. Rev. B* **2005**, *71*, 165434.
(2) Lehtinen, K. E. J.; Zachariah, M. R. *Phys. Rev. B* **2001**, *63*, 205402.
(3) Friedlander, S. K. *Smoke, Dust and Haze: Fundamentals of Aerosol Dynamics*; Oxford University Press: New York, 2000.
(4) Lu, P. J.; Conrad, J. C.; Wyss, H. M.; Schofield, A. B.; Weitz, D. A. *Phys. Rev. Lett.* **2006**, *96*, 028306.
(5) Russel, W. B. Saville, D. A., Schowalter, W. R. *Colloidal Dispersions*; Cambridge University Press: New York, 1989.
(6) Chokshi, A.; Tielens, A. G. G. M.; Hollenbach, D. *Astrophys. J.* **1993**, *407*, 806–819.
(7) Israelachvili, J. *Intermolecular and Surface Forces*; Academic: San Diego, CA, 1992.
(8) Parsegian, V. A. *Van der Waals Forces*; Cambridge University Press: Cambridge, U.K., 2006.
(9) Yannopapas, V.; Vitanov, N. V. *Phys. Rev. Lett.* **2007**, *99*, 120406.
(10) Yannopapas, V. *Phys. Rev. B* **2007**, *76*, 235415.
(11) Lifshitz, E. M. *Sov. Phys. JETP* **1956**, *2*, 73.
(12) Domingues, G.; Volz, S.; Joulain, K.; Greffet, J. J. *Phys. Rev. Lett.* **2005**, *94*, 085901.
(13) Pérez-Madrid, A.; Rubí, J. M.; Lapas, L. C. *Phys. Rev. B* **2008**, *77*, 155417.
(14) Narayanaswamy, G.; Chen, G. *Phys. Rev. B* **2008**, *77*, 075125.
(15) Volokitin, I.; Persson, B. N. J. *Phys. Rev. B* **2002**, *65*, 115419.
(16) Blanton, S. A.; Leheny, R. L.; Hines, M. A.; Guyot-Sionnest, P. *Phys. Rev. Lett.* **1997**, *79*, 865.
(17) Li, L. S.; Alivisatos, A. P. *Phys. Rev. Lett.* **2003**, *90*, 097402.
(18) Shim, M.; Guyot-Sionnest, P. *J. Chem. Phys.* **1999**, *111*, 6955.
(19) Shanbhag, S.; Kotov, N. A. *J. Phys. Chem. B* **2006**, *110*, 12211.
(20) Talapin, D. V.; Shevchenko, E. V.; Murray, C. B.; Titov, A. V.; Kral, P. *Nano Lett.* **2007**, *7*, 1213.
(21) Cho, K. S.; Talapin, D. V.; Gaschler, W.; Murray, C. B. *J. Am. Chem. Soc.* **2005**, *127*, 7140.
(22) Chen, X.; Mao, S. S. *Chem. Rev.* **2007**, *107*, 2891.
(23) Pratsinis, S. E. *Prog. Energy Combust. Sci.* **1998**, *24*, 197.
(24) Zhao, B.; Uchikawa, K.; McCormick, J. R.; Ni, C. Y.; Chen, J. G.; Wang, H. *Proc. Combust. Inst.* **2005**, *30*, 2569.
(25) Thimsen, E.; Biswas, P. *AIChE* **2007**, *53*, 1727.
(26) Thimsen, E.; Rastgar, N.; Biswas, P. *J. Phys. Chem. C* **2008**, *112*, 4134.
(27) Matsui, M.; Akaogi, M. *Mol. Simul.* **1991**, *6*, 239.
(28) Naicker, P. K.; Cummings, P. T.; Zhang, Z. H.; Banfield, J. F. *J. Phys. Chem. B* **2005**, *109*, 15243.
(29) Koparde, V. N.; Cummings, P. T. *J. Phys. Chem. B* **2005**, *109*, 24280.
(30) Smith, W.; Forester, T. R. *J. Mol. Graphics* **1996**, *14*, 136–141.
(31) Smith, W.; Yong, C. W.; Rodger, P. M. *Mol. Simul.* **2002**, *28*, 385–471.
(32) Tang, Z. Y.; Zhang, Z. L.; Wang, Y.; Glotzer, S. C.; Kotov, N. A. *Science* **2006**, *314*, 274.
(33) Shytov, A. V.; Pustilnik, M. *Phys. Rev. B* **2007**, *76*, 041401(R).
(34) Ohara, P. C.; Leff, D. V.; Heath, J. R.; Gelbart, W. M. *Phys. Rev. Lett.* **1995**, *75*, 3466.
(35) Ackler, H. D.; French, R. H.; Chiang, Y. M. *J. Colloid Interface Sci.* **1996**, *179*, 460.
(36) Jackson, J. D. *Classical Electrodynamics*, 3rd ed.; Wiley: New York, 1999.
(37) Humphrey, W.; Dalke, A.; Schulten, K. *J. Mol. Graph.* **1996**, *14*, 33.

JP102750K